Heat Transfer in a Micro-actuator Operated by Radiometric Phenomena

Joong-Sik Heo
Researcher, Institute of Advanced Machinery and Technology, Sungkyunkwan University, 300 Chunchun-dong, Jangan-ku, Suwon 440-746, Korea
Young-Kyu Hwang*
Professor, School of Mechanical Engineering, Sungkyunkwan University, 300 Chunchun-dong, Jangan-ku, Suwon 440-746, Korea

The heat transfer characteristics of rarefied flows in a micro-actuator are studied numerically The effect of Knudsen number (Kn) on the heat transfer of the micro-actuator flows is also examined The Kn based on gas density and characteristic dimension is varied from near-continuum to highly rarefied conditions Direct simulation Monte Carlo calculations have been performed to estimate the performance of the micro-actuator. The results show that the magnitude of the temperature jump at the wall increases with Kn Also, the heat transfer to the isothermal wall is found to increase significantly with Kn

Key Words : Micro-Actuator, Radiometric Phenomena, DSMC Method, Rarefied Gas Flow Field, Knudsen Number

Nomenclature

a . Acceleration
A . Area
c . Velocity
f . Force
H : Vane height
k . Boltzmann constant
Kn : Knudsen number
L : Characteristic dimension
m : Mass
n Number density
N . Number of molecules; molecular number flux
p . Pressure
q Heat flux
R : Gas constant
R_f : Random number
t . Time
T Temperature

Greek symbols

ε : Energy of molecules
λ Mean free path
ς Degrees of freedom

Subscripts

i : Incident
o : Reference
r : Reflected
rot Rotational
tr Translational
x : x-direction

* Corresponding Author,
E-mail : ykhwang@yurim.skku.ac.kr
TEL : +82-31-290-7437, **FAX** : +82-31-290-5849
Professor, School of Mechanical Engineering, Sungkyunkwan University, 300 Chunchun-dong, Jangan-ku, Suwon 440-746, Korea (Manuscript **Received** March 22, 2004, **Revised** December 13, 2004)

1. Introduction

The field of micro-electro-mechanical systems (MEMS) has rapidly been developed during the last several years. From biomedical applications to flow control devices, the potential of MEMS has attracted the attention of many scientists and engineers The advances in fabrication techniques have enabled the production of micro-devices,

such as micro-actuators, micro-refrigerators, and micro-engines The characteristic length scales that govern the momentum and energy transport between MEMS and their environments are typically of the order of microns With the increasing demand of micro-devices, it is of great importance to understand the behavior of micro-fluid flows (Ho and Tai, 1996)

The scaling from the macro to micro domain is such that some forces that would not be appropriate to power larger devices can be very useful for operating micro-devices As an example, gas dynamic forces are an efficient means to power MEMS (Kennard, 1938 , Wadsworth and Muntz, 1996 , Ota and Kawata, 1994) Crookes' radiometer generates useful work or force due to the gas motion that develops on a surface maintained at a different temperature than a surrounding ambient rarefied gas (Wadsworth et al., 1994) In this study, the performance of micro-actuator utilizing radiometric forces is studied numerically

A schematic diagram of the micro-actuator proposed by Wadsworth and Muntz (1996) is shown in Fig 1 The cavity contains a chevron pattern of inclined vanes. The vane surfaces or the cavity boundaries are radiatively or resistively heated The vanes can be considered analogous to pistons, with local heating of a vane surface leading to a radiometric force that displaces the connecting rod Figure 1 shows the force direction on the actuator for the case where the surface 4 is heated

In this study, the heat transfer characteristics of two-dimensional micro-actuator flows are examined Direct simulation Monte Carlo (DSMC) calculations have been performed to estimate the performance of the micro-actuator In the present DSMC method, the interaction between molecules is modeled by the inelastic collision model Particularly, the effect of the gas rarefaction on the wall heat flux is investigated Simulation results are also compared with the previously known numerical results (Wadsworth and Muntz, 1996)

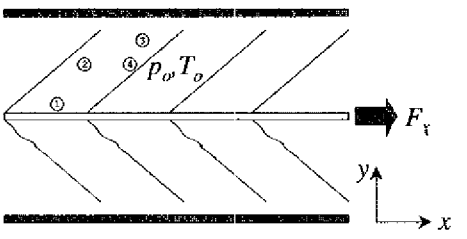

Fig. 1 Linear micro-actuator

2. Numerical Method and Actuator Geometry

2.1 DSMC method and boundary conditions

The Navier-Stokes equations based on the continuum model are applicable to numerous flow situations The model ignores the molecular nature of gases and liquids and regards the fluid as a continuous medium It is valid when the molecular mean free path (λ) is much smaller than the characteristic dimension (L) The ratio between the mean free path and the characteristic length is known as the Knudsen number ($Kn=\lambda/L$) and is used to indicate the degree of flow rarefaction All continuum models break down at sufficiently high Knudsen number and must be replaced by molecular models In the high Knudsen number flow regime, the linear relation between stress and rate of strain and the no-slip velocity condition are no longer valid for the Newtonian fluid Similarly, also, the linear relation between heat flux and temperature gradients and the no-jump temperature condition at the wall are no longer accurate

For $Kn \leq 0.01$, the flow is considered to be in the continuum regime and the Navier-Stokes equations are applicable Generally, when $Kn \geq 0.01$, the rarefaction effect tends to be significant For MEMS flow, Kn is large even at atmospheric operating conditions Therefore, conventional computational fluid dynamics (CFD) methods that are based on continuum assumptions may not be appropriate A method based on kinetic gas theory is required to describe the flows accurately (Bird, 1994)

The DSMC method is a well-established method for modeling flow for $Kn \geq 0.01$ (Bird, 1994) It computes the trajectories of a large number of

particles and calculates macroscopic quantities by sampling particle properties. In the present DSMC method, the interaction between molecules is modeled by the variable hard sphere (VHS) scattering assuming an inverse-power interatomic potential. The no time counter method is used as a collision sampling technique. The VHS model lead to a power law temperature dependence of the coefficient of viscosity. The temperature exponent ω ($\mu \propto T^{\omega}$) of nitrogen is chosen to be 0.74 with the reference molecular diameter of 4.17×10^{-10} m at the reference temperature 273 K (Bird, 1994). Also, chemical reactions and vibrational mode are assumed to be frozen. For the calculation of the rotational energy exchange between the colliding molecules, the Larsen-Borgnakke phenomenological model (1975) is employed.

Particles impinging on solid walls are reflected diffusely with full thermal and momentum accommodation. In the diffuse reflection model, the emission of the impinging molecules is not correlated with the pre-impinging state of the molecules. The outgoing velocity is randomly assigned according to a half-range Maxwellian distribution determined by the wall temperature.

2.2 Actuator geometry

The computational model of the actuator and the computational grid system are shown in Figs. 2(a) and (b), respectively. Geometric parameters and flow conditions are given in Table 1. The grid consists of uniform cells with 40×40 in the x and y directions. The number of simulated particles is 200,000. The time step must be small compared to mean collision time between molecules. Therefore, time step $\Delta t=2.5\times10^{-11}$ s was chosen at $Kn=0.027$ (case 1). The intermolecular collision number at each time step is about 2.3×10^{4}. In the process of simulation, the flow field is allowed to be developed with time. When the steady state is reached, the sampling of the molecules is started. The flow is sampled after each fourth time step. The results are based on time-averaged sampling over the time step from 200,000 to 400,000. The present DSMC simulation takes approximately 96 h of run time to obtain a converged solution for $Kn=0.027$.

Table 1 Simulated cases and conditions

Quantity	Case 1	Case 2	Case 3	Case 4	Case 5
H [μm]	2.0	1.0	0.5	0.1	0.05
l [μm]	2.0	1.0	0.5	0.1	0.05
θ [deg]	45				
p_o [kPa]	101.5				
T_o [K]	300				
Kn	0.027	0.054	0.108	0.54	1.08

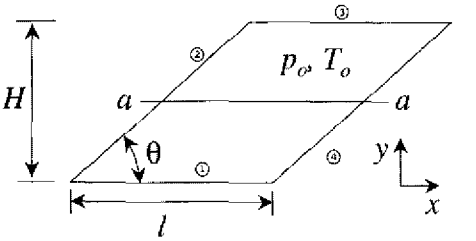

(a) Computational model of a micro-actuator. $a-a$ is a cross section at $H/2$

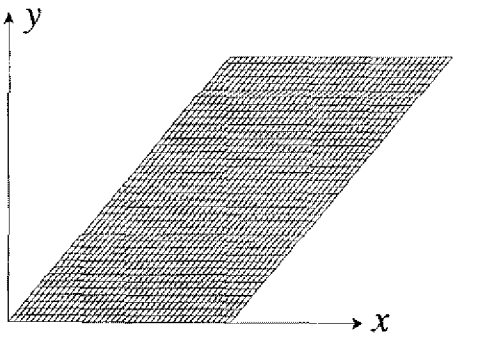

(b) Computational grid system

Fig. 2 Micro-actuator

A gas of undisturbed pressure p_o (1 atm) and temperature T_o (300 K) is confined between horizontal upper and lower cavity surfaces 1 and 3, and inclined vane surfaces 2 and 4. The model is symmetrical about surface 1 and is two-dimensional, which is an accurate assumption for the case where the vane width is much larger than the height H.

The variation of Kn is achieved by varying the vane height H, while keeping the ratio of vane height to separation distance l constant. The surfaces 1, 2, and 3 are kept at the undisturbed temperature 300 K, while the surface 4 is kept at 600 K.

2.3 Temperature and heat transfer

For equilibrium gases of diatomic molecules, by neglecting the vibrational energy, the temperature can be calculated as

$$T=(3T_{tr}+\zeta_{rot}T_{rot})/(3+\zeta_{rot}) \tag{1}$$

where T_{tr} denotes the translational temperature and T_{rot} represents the rotational temperature, respectively, ζ_{rot} is the number of rotational degrees of freedom (Bird, 1994). The translational and rotational temperatures are

$$\frac{3}{2}KT_{tr}=\overline{mc^2}-mc_o^2=\varepsilon_{tr} \tag{2}$$

$$T_{rot}=(2/k)(\overline{\varepsilon_{rot}}/\zeta_{rot}) \tag{3}$$

where k is the Boltzmann constant, m is the mass of a molecule, c is the velocity of a molecule, c_o is the mean velocity of simulated molecules, ε_{tr} and ε_{rot} are the translational and rotational energy of an individual molecule, respectively (Bird, 1994) The overbar in the above equations represents sample average

For nitrogen, there are two degrees of rotational freedom

$$\zeta_{rot}=2 \tag{4}$$

$$\varepsilon_{rot}=-\ln(R_f)kT \tag{5}$$

where R_f is a single random fraction

The net heat flux on a wall can be evaluated as

$$q=\frac{[(\sum\varepsilon_{tr}+\sum\varepsilon_{rot})_i-(\sum\varepsilon_{tr}+\sum\varepsilon_{rot})_r]N_o}{\Delta t\cdot A} \tag{6}$$

where the subscripts i and r denote the values before and after the impact of molecules on the wall; N_o is the real number of molecules associated with a computational molecule, Δt is the time step of sampling, A is the area (Bird, 1994)

3. Results and Discussion

The flows in a micro-actuator with the Knudsen number ranging from 0 027 to 1 08 have been simulated. Geometric parameters and flow conditions are given in Table 1 The lowest value of Kn=0 027 (case 1) is close to the continuum regime, while Kn=0 54 and 1 08 (cases 4 and 5) are in the highly rarefied regime

Table 2 Comparison of the present axial force f_x with the previous ones

	H=0 1 μm	H=1 μm	H=10 μm
Wadsworth & Muntz (1996)	0 068	0 027	0 006
Present	0 06821	0 02702	0 00596

Table 3 Effect of the time step Δt on the normalized axial force f_x for H=1 μm (case 2)

Time step (s)	f_x
$3\,7\times10^{-7}$	0 01022
$9\,7\times10^{-8}$	0 02104
$3\,1\times10^{-8}$	0 02529
$9\,5\times10^{-9}$	0 02704
$2\,8\times10^{-9}$	0 02690
$8\,5\times10^{-10}$	0 02700
$1\,4\times10^{-10}$	0 02711
$2\,5\times10^{-11}$	0 02709

To validate our computer program, the present numerical results are compared with the previously known numerical ones obtained by Wadsworth and Muntz (1996) for the elastic model The computations are conducted for the three different cases of H The present results agree well with those of Wadsworth and Muntz (1996), as shown in Table 2 For Kn=0 054 (case 2), Table 3 shows the effect of the time step Δt on the numerical results The axial force f_x is nearly constant if the time step is smaller than $2\,5\times10^{-11}$ s The force is normalized by the value p_oH The gas molecules exert a force on the surface 1, 2, 3, and 4 The value f_x is obtained by

$$f_x=\frac{[(\sum mc_x)_i-(\sum mc_x)_r]}{\Delta t\cdot p_o\cdot H} \tag{7}$$

where c_x is the x-component of velocity of molecules

3.1 *Effects of collision model*

The previous study (Wadsworth and Muntz, 1996) was conducted by employing the elastic collision model But, in the present study, the interaction between molecules is modeled by the

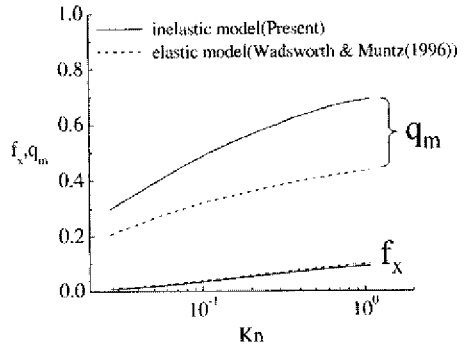

Fig. 3 Total axial force f_x and maximum average surface heat flux q_m versus Knudsen number

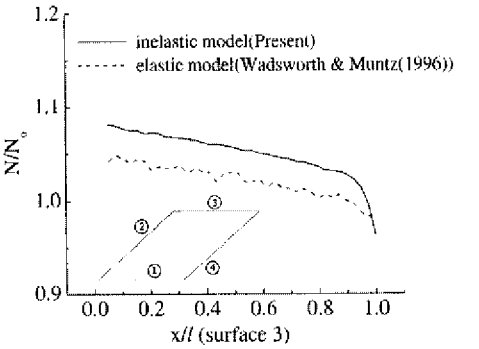

Fig. 4 Incident number flux on a surface 3 at $Kn=0.54$

inelastic collision model. The present numerical results are compared with those obtained by Wadsworth and Muntz (1996) in Fig. 3, where q_m is the maximum heat flux normalized by the product of the ambient pressure p_o and the speed of sound a_o. The value q_m occurs at the surface 3. For the normalized axial force f_x, good agreement between both results can be seen. However, there is a noticeable difference between both results for q_m. Namely, the difference is about 59% at $Kn=1.08$. As Kn increases, the discrepancy between both results becomes larger. This indicates that the elastic model is inappropriate for the heat transfer analysis of highly rarefied flows. The radiometric force increases as Kn increases (Kennard, 1938; Ota and Kawata, 1994; Wadsworth et al., 1994; Wadsworth and Muntz, 1996). It can be seen that f_x increases with Kn due to the radiometric effect. Also, the heat flux q_m increases with Kn. The increase of the number rate of molecules that impact the wall is apparently a dominant factor, contributing to the observed increase of the wall heat transfer rate.

Figure 4 shows the incident molecular number flux on the surface 3 at $Kn=0.54$. The number flux N is normalized by N_o,

$$N_o=\frac{1}{4}\, n_o\sqrt{\frac{8RT_o}{\pi}} \tag{8}$$

in which n_o is the number density and R is the gas constant, respectively (Bird, 1994). The value N_o is the inward number flux to the wall for a stationary equilibrium gas. For both models, N decreases along the vane surface. Also, it can be seen that N corresponding to the inelastic model is larger than that corresponding to the elastic model. Consequently, it causes the increase of the heat transfer rate q_m, as seen in Fig. 3. For both models, the incident molecular number flux on the surface 3 decreases along the surface. The incident number flux predicted by the inelastic model decreases rapidly at $x/l=1.0$. This is because the number of sampled molecules is very small at that location.

3.2 Number flux, temperature, and heat flux distributions

The distributions of the incident number flux N on surfaces 2 and 4 for various Kn are shown in Figs. 5(a) and (b), respectively. It can be seen that N on the surface 4, at the same x/l and Kn, is much smaller than that on the surface 2. Since the temperature of the surface 4 is 2 times larger than that of the other surfaces, the number density near the wall becomes smaller. It causes the decrease of N on the surface 4. Specifically, for the case of $Kn=0.027$, the normalized value of N/N_o on the surface 4 is much smaller than that on the surface 2.

Figure 6 shows the temperature distributions at section $a-a$ (see Fig. 2). As Kn increases, the degree of the temperature jump at the wall surface increases. Also, it can be seen that the degree of the temperature jump for the hot surface 4 is larger than that for the cool surface 2. The degree of the temperature jump is proportional to the temperature gradient at the wall

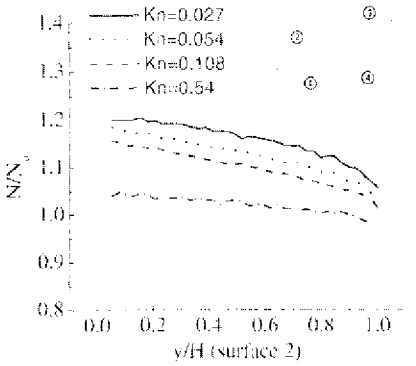

(a) Surface 2

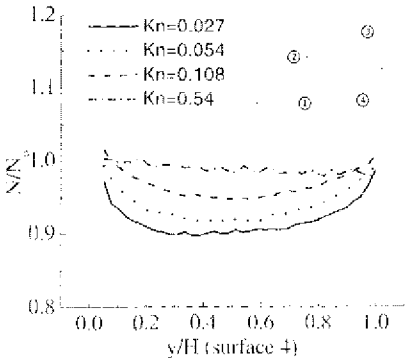

(b) Surface 4

Fig. 5 Incident number flux; The arrows indicate increasing Kn

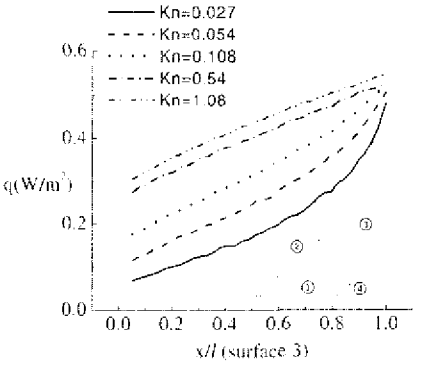

(a) Surface 3

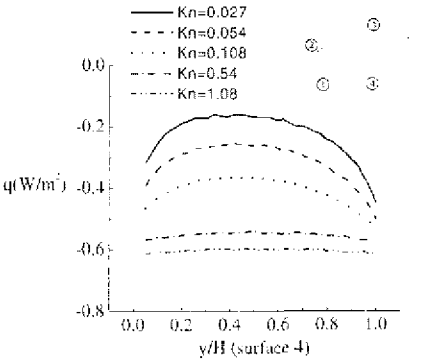

(b) Surface v*h*

Fig. 7 Heat flux distributions: The arrows indicate increasing Kn

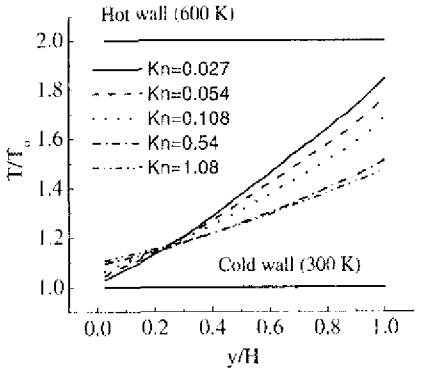

Fig. 6 Temperature distributions at various Knudsen number. The arrow indicates decreasing Kn

(Kennard, 1938). Thus,

$$T_{gas}-T_{wall}\propto\frac{\partial T}{\partial n} \tag{9}$$

where T_{gas} is the gas temperature and T_{wall} is the wall temperature; n is the coordinate perpendicular to the wall. The temperature gradient at the hot surface is larger than that at the cool surface.

The heat flux distributions as a function of Kn at surfaces 3 and 4 are shown in Figs. 7(a) and (b), respectively. It can be seen that the heat flux increases with the Kn. For the surface 4, since the heat is removed from the surface, the sign of the heat flux is negative.

3.3 Calculation of the axial force of an actuator

As seen in Fig. 3, the normalized axial force f_x increases with Kn due to the radiometric effect. For a vane height of $H=1$ μm (i.e., $Kn=0.054$), f_x is 0.0173. Therefore, the axial force per vane is

$$\tilde{F}_x=f_x p_o H=1.756\times10^{-8}\ \text{N/m}. \tag{10}$$

For the case of the number of vanes n_v and the

vane width $w=100\ \mu m$, the total available force F_x is

$$F_x=\tilde{F}_x \cdot n_v w=8.78\times10^{-6}\ \mathrm{N} \tag{11}$$

Neglecting friction of the linkage support points, the net force F_x provides an actuator acceleration $a=F_x/m=1.756\times10^{6}\ \mathrm{m/s^2}$, where m $(=5\times10^{-12}\ \mathrm{kg})$ is the mass of the actuator (Wadsworth and Muntz, 1996). Assuming a to be constant, the time to move a distance x can be calculated by

$$t_x=\sqrt{2x/a} \tag{12}$$

Therefore, we can see that the time to move a distance $x=1$ mm is 33.7 μs.

3.4 Distributions of the rarefied flow field

Velocity vectors, shown in Figs. 8(a)~(e),

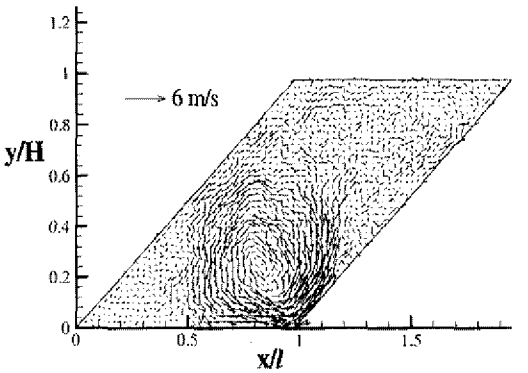

(a) $Kn=0.027$ $(H=2\ \mu m)$

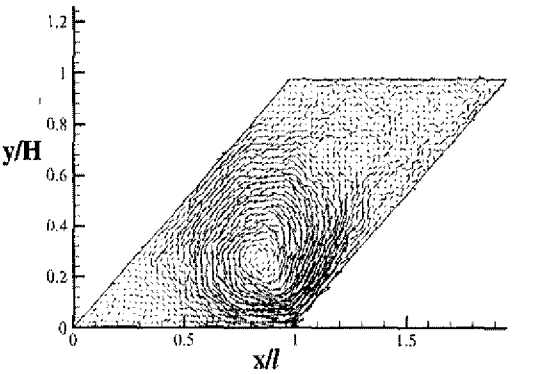

(b) $Kn=0.054$ $(H=1\ \mu m)$

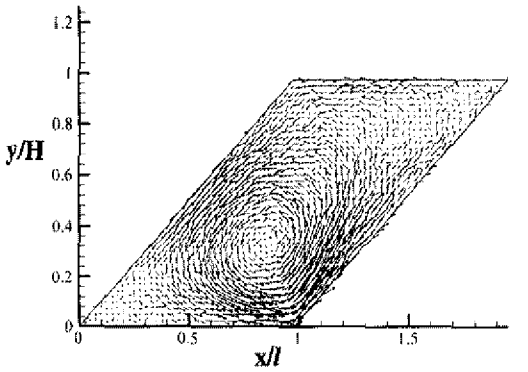

(c) $Kn=0.108$ $(H=0.5\ \mu m)$

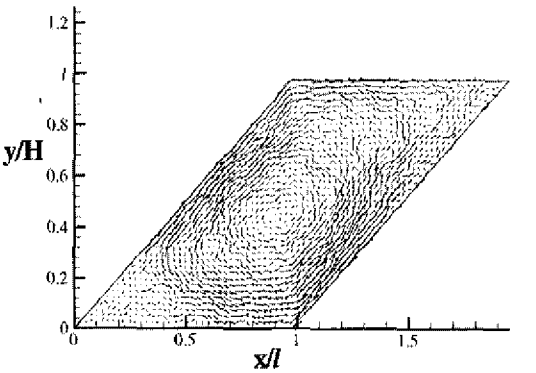

(d) $Kn=0.54$ $(H=0.1\ \mu m)$

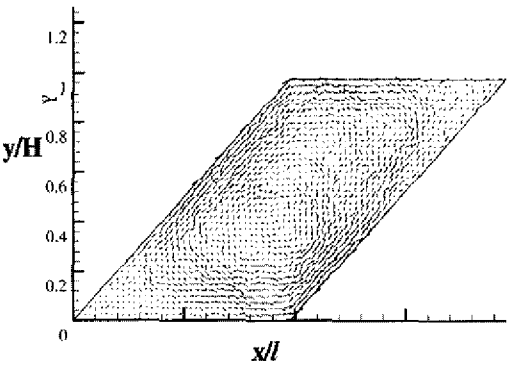

(e) $Kn=1.08$ $(H=0.05\ \mu m)$

Fig. 8 Velocity vectors

show how the flow changes with Kn. They show the swirling motion developed by the radiometric effects in the originally stationary gas. The gas flows are induced by the temperature difference between surfaces. The radiometric phenomena are due to the thermal creep of the gas over an unequally heated surface (Kennard, 1938). This flow pattern has been observed by Ota and Kawata (1994) for a micro engines. The peak value of the velocity occurs at the hot surface 4. As Kn increases, the location of the vortex center moves up.

Figure 9 shows the temperature contours. Because of the presence of significant temperature jump, the temperature near the hot wall decreases as Kn increases. Figure 10 shows the number density contours, and the density near the hot wall increases as Kn increases.

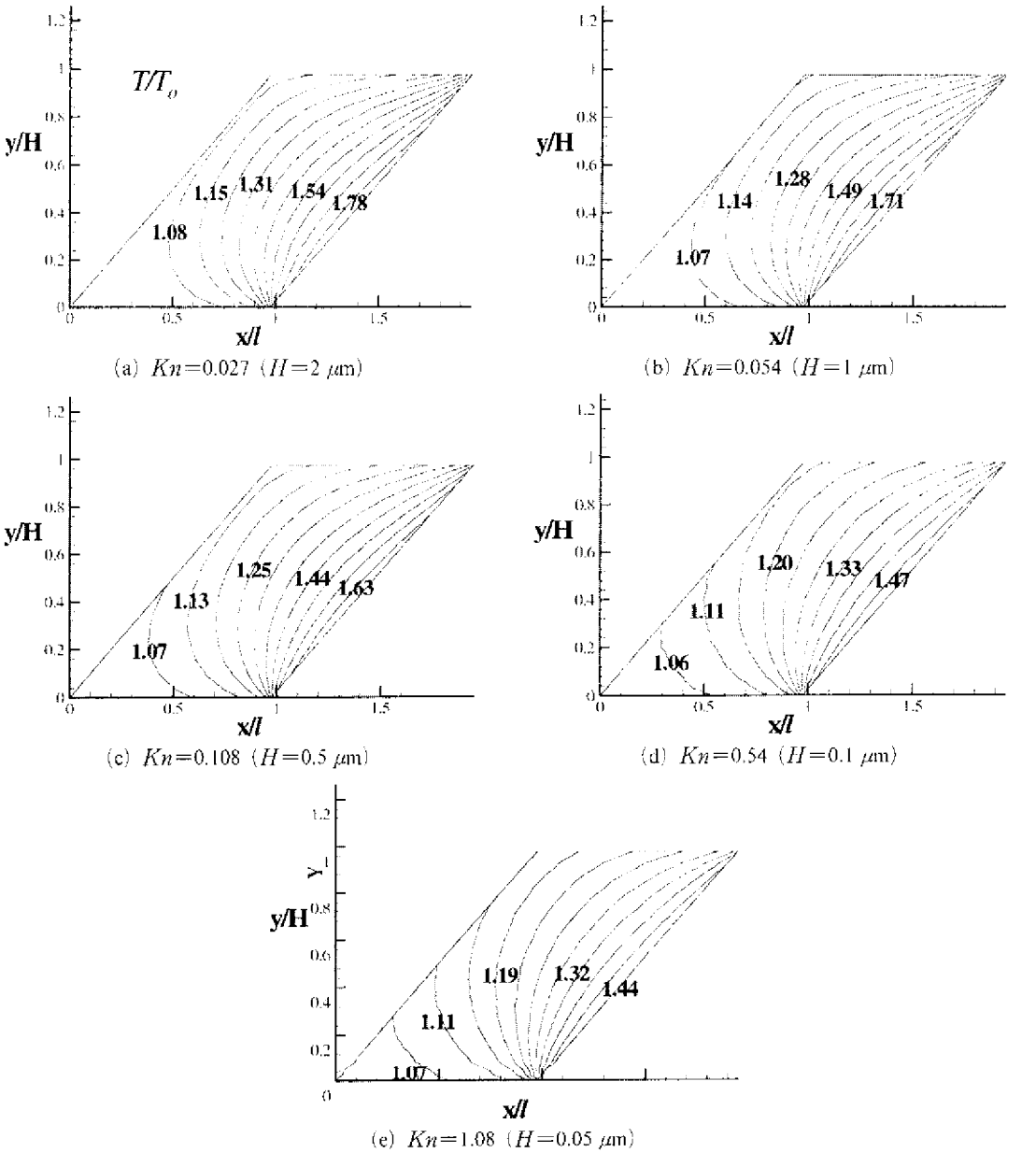

(a) Kn=0.027 (H=2 μm) (b) Kn=0.054 (H=1 μm)

(c) Kn=0.108 (H=0.5 μm) (d) Kn=0.54 (H=0.1 μm)

(e) Kn=1.08 (H=0.05 μm)

Fig. 9 Temperature contours

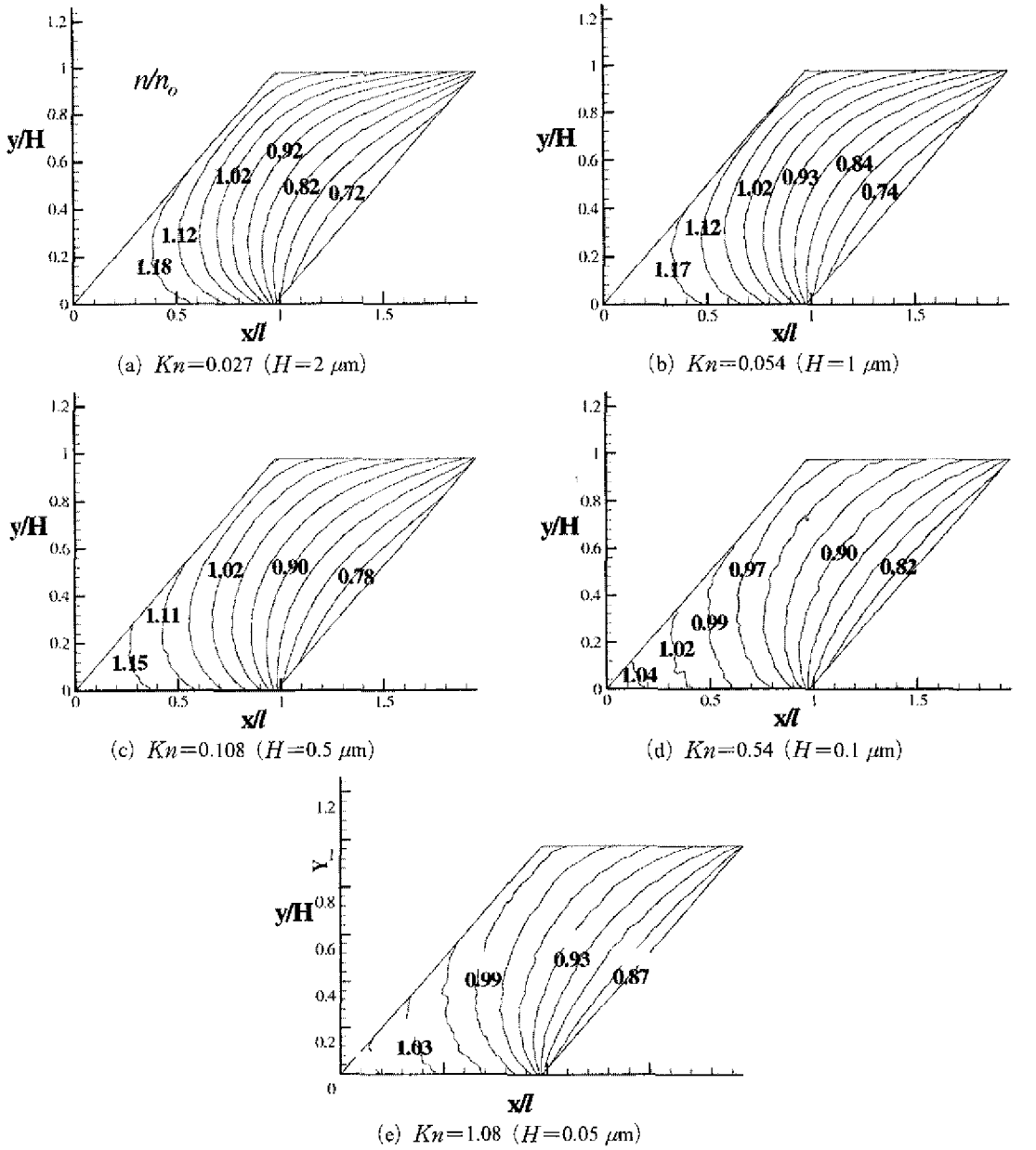

(a) Kn=0.027 (H=2 μm) (b) Kn=0.054 (H=1 μm)

(c) Kn=0.108 (H=0.5 μm) (d) Kn=0.54 (H=0.1 μm)

(e) Kn=1.08 (H=0.05 μm)

Fig. 10 Density contours

4. Conclusions

A linear micro-actuator powered by radiometric gas dynamic forces has been analyzed. Direct simulation Monte Carlo calculations have been performed to estimate the performance of the micro-actuators.

The results show that the heat transfer characteristics of the micro-actuator flows can vary significantly with the Knudsen number. For the two-dimensional rarefied flows in the micro-actuator, there is a significant increase of the wall heat transfer with the Knudsen number. It can be seen that the axial force of the actuator increases with the Knudsen number due to the radiometric effect. Also, the simulation results show that there is a swirling motion developed by the radiometric

effects in the gas

Acknowledgment

This work was supported by grant No KRF-2003-041-D20098 from the Korea Research Foundation

References

Bird, G A, 1994, *Molecular Gas Dynamics and the Direct Simulation of Gas Flows*, Clarendon Press, Oxford

Borgnakke, C and Larsen, P S, 1975, "Statistical Collision Model for Monte Carlo Simulation of Polyatomic Gas Mixture," *J Comput Phys*, Vol 18, pp 405~420

Ho, C M and Tai, Y C, 1996, "REVIEW MEMS and Its Applications for Flow Control," *J Fluids Eng*, Vol 118, 437~447

Kennard, E H, 1938, *Kinetic Theory of Gases*, McGraw-Hill

Ota, M and Kawata, N, 1994, "Direct Simulation of Gas Flows around Rarefied Gas Dynamics Engines for a Micro-Machine," *Proc 19th Int Symp on Rarefied Gas Dynamics*, Oxford, pp 722~728

Wadsworth, D C, Muntz, E P, Pham-Van-Diep, G and Keeley, P, 1994, "Crookes' Radiometer and Micromechanical Actuators," *Proc. 19th Int. Symp. on Rarefied Gas Dynamics*, Oxford, pp 708~714

Wadsworth, D C and Muntz, E P, 1996, "A Computational Study of Radiometric Phenomena for Powering Microactuators with Unlimited Displacements and Large Available Forces," *J Microelectromechanical Syst*, Vol 5, No 1, pp 59~65